Journal of Porphyrins and Phthalocyanines
J. Porphyrins Phthalocyanines 2013; **17**: 92–98
DOI: 10.1142/S1088424612501313

Published at http://www.worldscinet.com/jpp/

Electrochemistry and spectroelectrochemistry of carboxyphenylethynyl porphyrins

Pei-Shang Chao, Ming-Yu Kuo, Chen-Fu Lo, Min-Hsu Hsieh, Yu-Hsiang Cheng, Chin-Li Wang, Hsiu-Yu Lu, Hshin-Hui Kuo, Yen-Ni Hsiao, Chieh-Ming Wang and Ching-Yao Lin*

Department of Applied Chemistry, National Chi Nan University, No. 302 University Road, Puli,
Nantou Hsien 54561, Taiwan

Received 23 July 2012
Accepted 1 October 2012

ABSTRACT: Zinc 5-(4-carboxy-phenylethynyl)-10,20-biphenylporphines bearing various substituents on the 10,20-phenyl rings are studied for their electrochemical and spectroelectrochemical properties. Cyclic voltammetry and optically transparent thin-layer electrochemical measurements suggest that the first reductions of these porphyrins should be the reduction reaction of the carboxylic protons. For the porphyrin ring reactions, our study shows that the redox properties can be significantly affected by the alkoxyl chains on the 10,20-phenyl rings.

KEYWORDS: porphyrin, electrochemistry, spectroelectrochemistry, carboxyphenylethyne.

INTRODUCTION

Dye-sensitized solar cells (DSSC) have drawn much attention because of the relatively high efficiencies, simple device design, and lower production cost [1–3]. Overall efficiencies (η) greater than 11% have been demonstrated with ruthenium dyes [4–6]. In recent years, other types of sensitizers have also been intensely studied. Among the dyes under investigation, porphyrins are considered as one of the more efficient sensitizers for DSSC applications because of the vital roles of porphyrin derivatives in photosynthesis, the strong UV-visible light absorption, and the ease of modifying their chemical structures [7–19]. In the development of porphyrin dyes, Officer and co-workers reported the overall efficiency of porphyrin-sensitized solar cells (PSSC) above 7% by using a side-anchoring, fully conjugated dye [10]. With the use of cobalt-based electrolyte and an organic co-sensitizer, the PCE of the PSSC device reached 12% recently [11a]. Independently, our systematic studies have yielded several highly efficient porphyrin dyes in the past [14–19], three of which showed overall efficiencies greater than 10% with the use of classic DSSC setup. It is worth noting that 4-carboxy-phenylethyne is often used as the anchoring group for the porphyrin dyes [8a, 11, 13–19], including many highly efficient ones [11, 17, 18]. However, only very basic electrochemistry of these porphyrins, such as the redox potentials, has been reported.

In this work, we aim to reveal more detailed electrochemical properties of zinc porphyrins modified with a 4-carboxy-phenylethynyl anchoring group. The porphyrins under investigation are denoted as PE1, PE1-OR6, and PE1-OR4 and their structures are shown in Chart 1. As shown in the chart, these porphyrins employ zinc biphenylporphine (ZnBPP) as the core chromophore and a 4-carboxy-phenylethyne as the anchoring substituent for DSSC applications. The differences in the structures of these porphyrins are the substituents on the 10,20-phenyl rings. For PE1, the phenyl groups are not further modified. For PE1-OR6, six dodecoxyl chains are added to the para- and meta-positions of the two phenyl rings. For PE1-OR4, four dodecoxyl chains are attached to the ortho-positions of the two phenyl groups. The dodecoxyl chains are introduced to increase the solubility of the porphyrin in the organic solvents.

---

*Correspondence to: Ching-Yao Lin, email: cyl@ncnu.edu.tw, tel: +886 49-2910960 ext. 4152, fax: +886 49-2917956

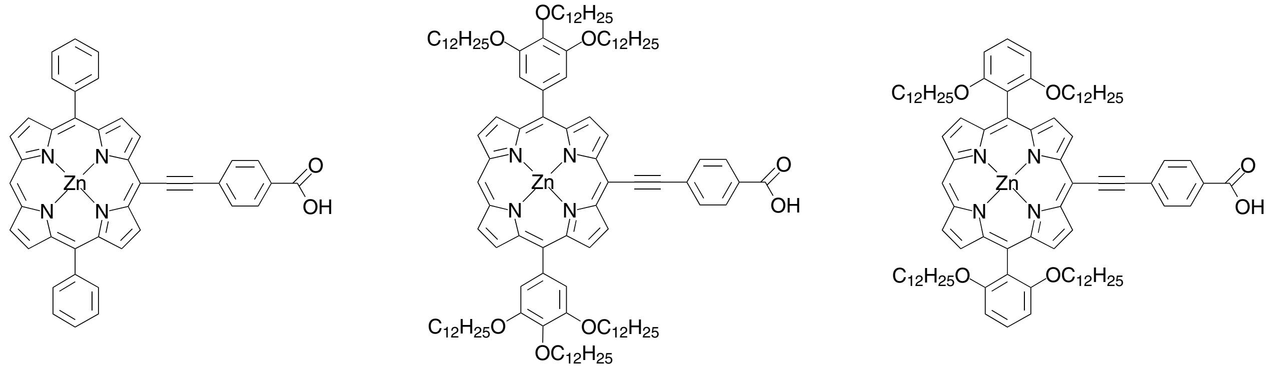

PE1 PE1-OR6 PE1-OR4

Chart 1. Structural diagram of the PE1 porphyrins under investigation

As we have recently reported, the positions of these long alkoxyl groups play a significant role in improving the photovoltaic performance of the PSSC [17]. Likewise, the positions of the long alkoxyl groups were also observed to significantly affect the electrochemical behaviors of the porphyrins.

EXPERIMENTAL

Materials

Air-sensitive solids were handled in an MBraun Unilab glove box. A vacuum line and standard Schlenk techniques were employed to process air-sensitive solutions. Tetrahydrofuran (THF) was obtained from Merck (Darmstadt, Germany). Other chemicals were ordered from Acros Organics (New Jersey, U.S.A.). THF and tetrabutylammonium perchlorate (TBAP) were were purified according to the literature methods [20]. The synthesis of PE1, PE1-OR6 and PE1-OR4 has been previously reported [14, 17]. Free-base PE1-OR4 was prepared by demetallating PE1-OR4 in $CHCl_3$ with $HCl_{(aq)}$. 100 mg PE1-OR4 was usually dissolved in 100 mL of $CHCl_3$ for the process. After adding 10 mL of 12 M $HCl_{(aq)}$, the solution was stirred at room temperature for 4 hours. The completion of the reaction was monitored by UV-visible spectrscopy and TLC techniques. Upon completion, the organic solution was first neutralized by three washes of $K_2CO_{3(aq)}$ followed by three washes of $NH_4Cl_{(aq)}$. After chromatographic separation on silica gel (with CH_2Cl_2/MeOH = 9/1) and crystalization from CH_2Cl_2/MeOH, 71% of free-base PE1-OR4 was collected. Characterization data: ^1H NMR (300 MHz $CDCl_3$ at 7.26 ppm): δ ppm 10.02 (s, 1H), 9.69 (d, J = 4.5 Hz, 2H), 9.16 (d, J = 4.8Hz, 2H), 8.92 (d, J = 4.5 Hz, 2H), 8.86 (d, J = 4.5 Hz, 2H), 8.30 (d, J = 8.0 Hz, 2H), 8.11 (d, J = 8.0, 2H), 7.71 (t, J = 8.4 Hz, 2H), 7.01 (d, J = 8.4 Hz, 4H), 3.85 (t, J = 6.5 Hz, 8H), 1.30–0.75 (m, 64H), 0.75–0.35 (m, 34H), -2.43 (s, 2H). Elemental analysis: $C_{89}H_{122}N_4O_6$, calcd. C 79.54%, H 9.15%, N 4.17%; found C 79.23%, H 9.31%, N 3.82%. Mass $[MH]^+$ calcd. 1342.94, found 1343.83.

Instrumentation

Absorption spectra were recorded on an Agilent 8453 UV-visible spectrophotometry system. A CH Instruments Electrochemical Workstation 611A was used to performed cyclic voltammograms and thin-layer electrolysis. Cyclic voltammetry was carried out with a standard three-electrode cell. The reference electrode (SCE) was isolated from the main compartment by a junction tipped with a platinum wire. Spectroelectrochemical results were measured with an air-tight, optically transparent thin-layer electrochemical (OTTLE) cell [21]. The cell is made of quartz with 1-mm in light path. The working electrode, constructed with a 100 mesh platinum gauze, was placed inside the cell, while the reference and counter electrodes were individually separated from the main compartment by a layer of fine glass frit. The electrochemical cells were all assembled in a glovebox equipped with a drytrain to exclude moisture and oxygen.

Molecular simulation

The molecular dynamics (MD) simulations of the porphyrins were carried out with the use of Materials Studio software package. Details of the simulation procedure have been previously published [17b]. To simplify the calculation, free-base porphyrins were used in these simulations.

RESULTS AND DISCUSSION

Figure 1 collects the cyclic voltammograms (CVs) of PE1 porphyrin, ZnBPP, 4-carboxy-phenylethyne (PE), and the blank solution (THF/0.1 M TBAP) under the same experimental conditions. The redox potentials are listed in Table 1. First of all, the reduction reaction of ZnBPP occurs at -1.40 V *vs* SCE as a quasi-reversible reaction (Fig. 1b). This potential is consistent with the formation

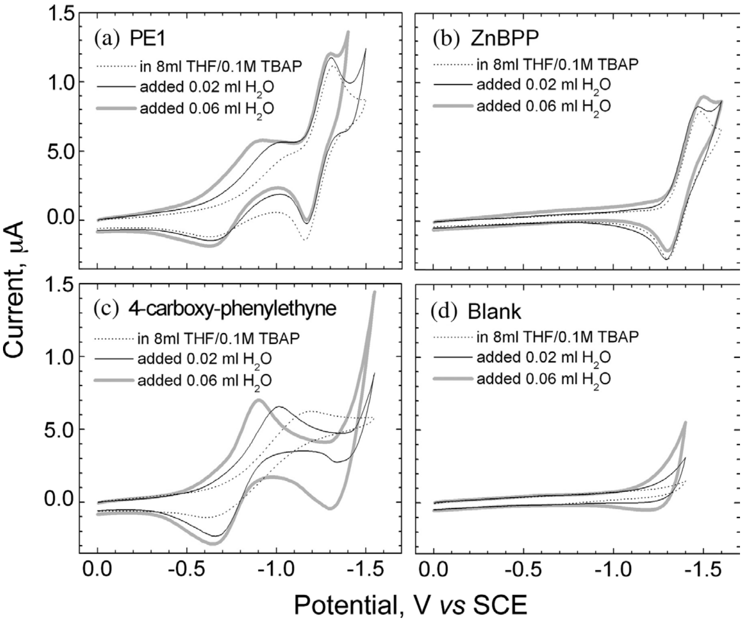

Fig. 1. Cyclic voltammograms of 1.0 mM (a) PE1, (b) ZnBPP, (c) 4-carboxy-phenylethyne (PE) in 8 mL THF/0.1 M TBAP solutions, and (d) the blank solutions (THF/0.1 M TBAP). The dotted lines represent the dried solutions, thin solid lines: added 0.02 mL H_2O (2.5%), and bold lines: added 0.06 mL H_2O (7.5%). This figure qualitatively demonstrates the effect of H_2O on the potential of PE1's first reduction reaction

Table 1. Reduction potentials of PE1, ZnBPP, and 4-carboxy-phenylethyne (PE)[a]

Entry	THF/0.1 M TBAP	Added H_2O (2.5%)	Added H_2O (7.5%)
PE1 (Red 1)	-0.86 V (450 mV)	-0.83 V (390 mV)	-0.78 V (300 mV)
PE1 (Red 2)	-1.24 V (160 mV)	-1.24 V (140 mV)	-1.24 V (130 mV)
ZnBPP	-1.40 V (190 mV)	-1.39 V (170 mV)	-1.40 V (200 mV)
PE	-0.91 V (570 mV)	-0.84 V (36 mV)	-0.78 V (250 mV)

[a] Reaction conditions: 1.0 mM of the compound in 8 mL THF/0.1 M TBAP; Pt working and counter electrodes; SCE reference electrode; scan rate = 100 mV/s. For $Fc^{+/0}$ in the same condition, $E_{1/2}$ = +0.49 V *vs* SCE. Peak-to-peak separations (mV) are put in the parentheses for the quasi-reversible reactions.

of a zinc porphyrin anion radical [22]. For PE1 porphyrin, two waves of reversible reductions were observed at -0.86 and -1.24 V *vs* SCE (Fig. 1a). Bulk electrolysis indicates that there are two electrons involved in these reduction reactions. In other words, there are two one-electron reduction reactions observed for PE1 porphyrin. Coulometric titration with the use of an OTTLE cell [21] agrees well with this suggestion (titration curves shown as insets in Fig. 2a and 2b). The first reduction of PE1 porphyrin is an ill-shaped, quasi-reversible reaction. Interestingly, the potential of this reaction is susceptible to the presence of H_2O in the system. As shown in Fig. 1a and Table 1, the redox potential of PE1's first reduction reaction is positively shifted from -0.86 V to -0.78 V *vs* SCE by increasing water content in the THF solution to 7.5% (v/v). A nearly identical phenomenon was also observed for the anchoring substituent, 4-carboxy-phenylethyne, under the same conditions (Fig. 1c). In contrast, the second reduction potential of PE1 porphyrin is not sensitive to the introduction of H_2O. Half-wave potential of ZnPE1's second reduction was observed at -1.24 V *vs* SCE. This value is consistent with the formation of a porphyrin anion radical. This potential is positively shifted from that of ZnBPP (-1.40 V) due to the more extended π-conjugation system of PE1 porphyrin [14]. As such, by comparing the CVs of PE1 with those of ZnBPP and 4-carboxy-phenylethyne, Fig. 1 indicates that the first reduction reaction of PE1 porphyrin should localize at the anchoring 4-carboxy-phenylethynyl group and the second reduction should occur at the porphine ring.

To further our understanding to the reduction reactions of PE1 porphyrin, spectroelectrochemical measurements were carried out with the use of an OTTLE cell in THF/TBAP under N_2. Figure 2 collects the UV-visible spectrum changes of PE1 porphyrin upon (a) the first reduction at -1.10 V *vs* SCE, (b) the second reduction at -1.40 V *vs* SCE, and (c) the acid-base titration by TBAOH. Coulometric titration (Fig. 2a and 2b insets) indicates that two reductions of PE1 are both one-electron transfer reactions. Upon the first reduction, the absorption bands of PE1 are slightly red-shifted and the absorption bands remain relatively sharp (Fig. 2a). Isosbestic points observed in this figure suggest that no intermediates were observed during the electrolysis. Intriguingly, these spectral changes are nearly identical to those of PE1 being titrated by TBAOH (Fig. 2c). Therefore, this figure strongly suggests that the first reduction of PE1 in THF/TBAP should involve deprotonation reaction of the 4-carboxy-phenylethynyl substituent, generating a localized anion at the anchoring group. This phenomenon is similar to changing a substituent at the porphyrin *meso*-position and observing slightly shifted sharp absorption bands. Upon the second reduction, the absorption bands of PE1 became very broadened and largely red-shifted at -1.40 V *vs* SCE (Fig. 2b). These spectrum changes are consistent with the formation of a porphyrin anion radical, *i.e.* a one-electron reduction at the porphine core [22].

It has been reported that benzoic acid undergoes one-electron reduction reaction in solutions, generating benzoate anion and hydrogen [23]. Based on this mechanism, we suggest that the carboxylic substituent of PE1 porphyrin loses one proton upon the first one-electron reduction

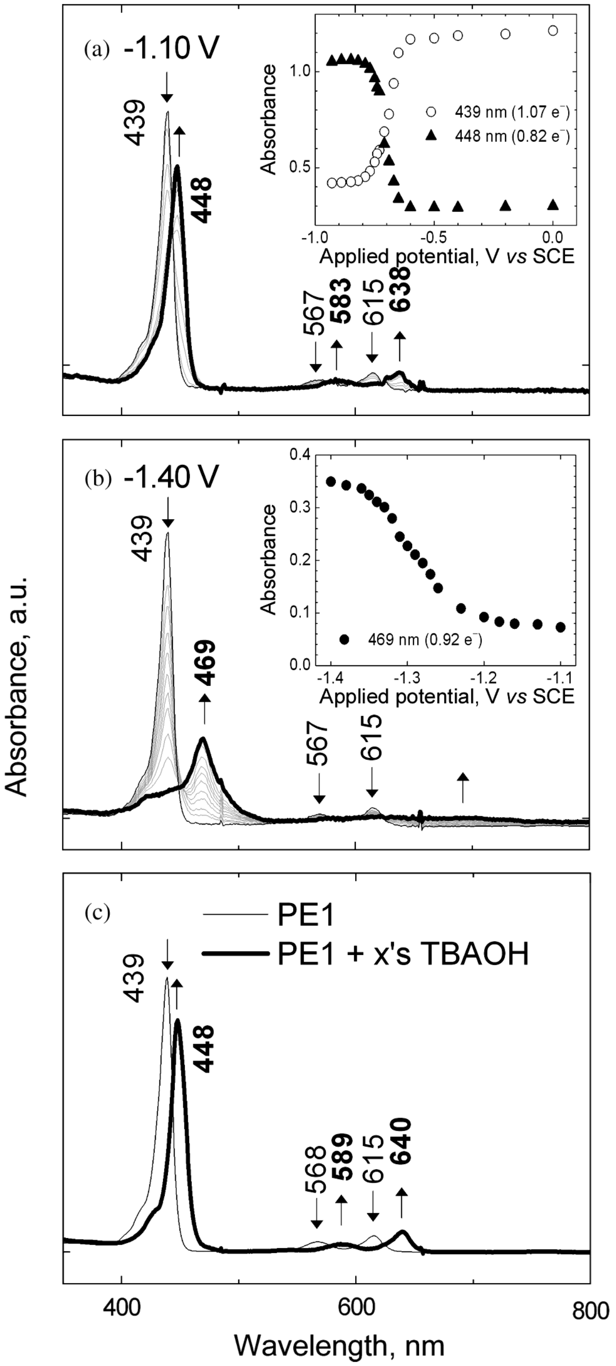

Fig. 2. Absorption spectrum changes of PE1 porphyrin in THF/0.5 M TBAP upon (a) the first one-electron reduction, (b) the second one-electron reduction, and (c) TBAOH titration. The insets show the coulometric titration curves

around -0.86 V *vs* SCE, yielding a carboxylate group and hydrogen. At -1.24 V *vs* SCE, the porphine core receives an additional electron and becomes a porphyrin anion radical. Scheme 1 illustrates this proposed mechanism. It is worth mentioning that it would be of great interests if the first reduction reaction of PE1 porphyrin were catalytical. That would translate to a possibility of continuous H_2 generation. Unfortunately, we did not observe catalytical generation of hydrogen at this time.

Figure 3 collects the CVs of PE1, PE1-OR6, and PE1-OR4 in THF/TBAP. The redox potentials are listed in Table 2. As shown in the figure and table, PE1 and PE1-OR6 behaves very similarly. The first porphine ring reductions are both *quasi*-reversible for PE1 (-1.24 V *vs* SCE) and PE1-OR6 (-1.27 V *vs* SCE). However, the first porphine ring oxidations appear to be irreversible reactions for PE1 (+1.04 V *vs* SCE) and PE1-OR6 (+1.08 V *vs* SCE). As for PE1-OR4, the first porphine ring reduction was observed at -1.47 V *vs* SCE as a *quasi*-reversible reaction. Interestingly, the first oxidation of PE1-OR4 was observed as a *quasi*-reversible reaction at +0.85 V *vs* SCE, in sharp contrast to the irreversible oxidation waves of PE1 and PE1-OR6 under the same condition. This phenomenon strongly suggests that six alkoxyl chains at the *meta*- and *para*-positions of the phenyl groups should have very limited influence to the porphyrin redox behaviors. On the contrary, four alkoxyl chains at the *ortho*-positions of the phenyl groups have a significant impact to the potentials as well as the reversibility of the redox reactions. These differences may be attributed to two possibilities. (a) The four alkoxyl chains at the *ortho*-positions of the PE1-OR4 phenyl groups are in the positions to have more electron-donating influence than are the six alkoxyl chains at the *meta*- and *para*-positions of the PE1-OR6 phenyl rings. (b) The spacial arrangement of PE1-OR4's four alkoxyl chains are in a shape of wrapping around the porphyrin core structure in the solution whereas PE1-OR6's six alkoxyl chains extend into the solution (see below).

In order to further our understanding to the differences in the electrochemical behaviors mentioned above, we performed molecular simulations on PE1-OR6 and PE1-OR4 by using Materials Studio software package [24]. Because of the long alkoxyl chains, obtaining crystal structures of the porphyrins is not feasible. More importantly, simulation results provide the opportunity of visualizing the alkoxyl chains in the solutions. To simplify

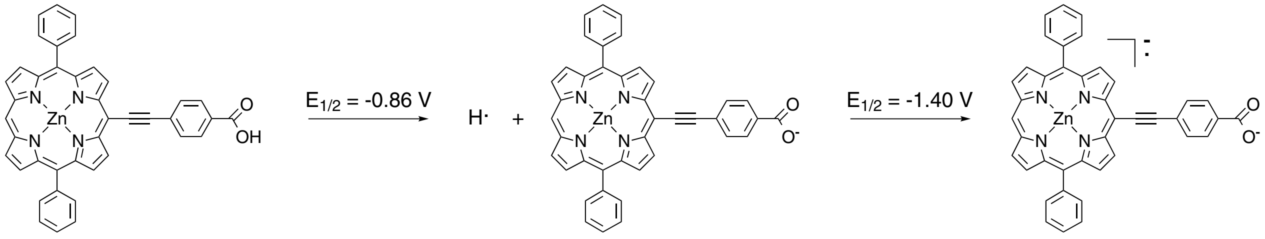

Scheme 1. Proposed mechanism of PE1 porphyrin reduction reactions. This suggested mechanism is based on reference [23]

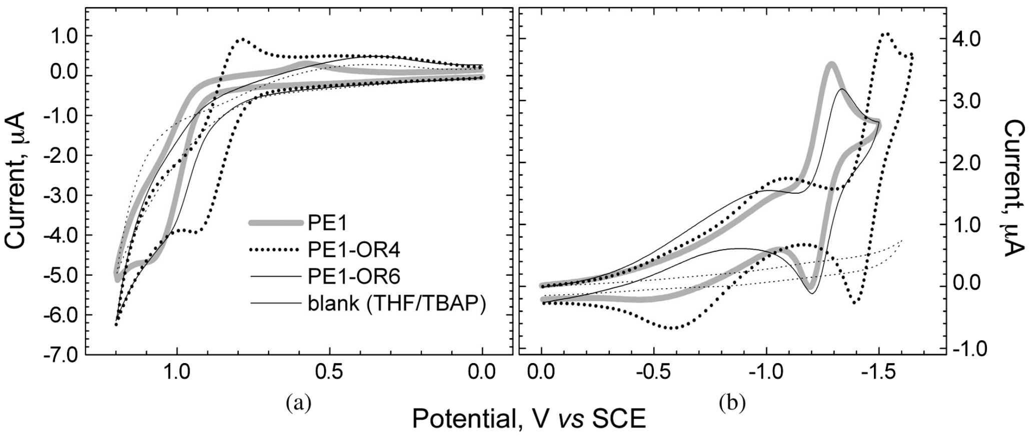

Fig. 3. Cyclic voltammograms of 1.0 mM of PE1 (grey lines), PE1-OR4 (bold dotted lines), and PE1-OR6 (thin solid lines) in THF/0.1 M TBAP (thin dotted lines) solutions

Table 2. Redox potentials of PE1, PE1-OR6, and PE1-OR4 porphine ring reactions[a]

	PE1	PE1-OR6	PE1-OR4	H_2PE1-OR4
Reduction	-1.24 (100)	-1.27 (140)	-1.47 (130)	-1.22 (140)
Oxidation	+1.08 (E_{pa})	+1.04 (E_{pa})	+0.85 (150)	+1.11[b]

[a] Reaction conditions: 1.0 mM of the porphyrin in THF/0.1 M TBAP; Pt working and counter electrodes; SCE reference electrode; scan rate = 100 mV/s. For $Fc^{+/0}$ in the same condition, $E_{1/2}$ = +0.49 V *vs* SCE. Peak-to-peak separations (mV) are put in the parentheses for *quasi*-reversible reactions. [b] This value is determined by differential pulse voltammetry because the reaction is too close to the detection limit to have a correct reading.

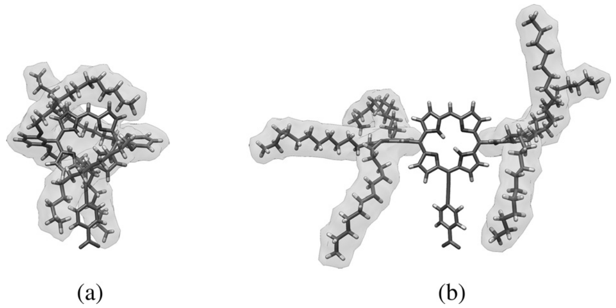

Scheme 2. Simulated molecular structures of (a) PE1-OR4 and (b) PE1-OR6 in solutions. The alkoxyl and alkyl chains are highlighted. Note that this scheme is to visualize the orientations of the long alkoxyl chains in the solutions

the calculation, free-base porphyrins were used in these simulations. The results are compared in Scheme 2. As shown in the scheme, the phenyl groups at the macrocyclic *meso*-positions are fairly perpendicular to the porphyrin macrocylic planes due to the steric hindrance between the porphine ring and the phenyl rings. As for the alkoxyl chains, the four dodecoxyl chains of PE1-OR4 are simulated to wrap around the porphine core whereas the six alkoxyl chains of PE1-OR6 are simulated to extend into the bulk solution. As mentioned above, the redox potentials of the first porphine reduction and oxidation of PE1-OR4 are both negatively shifted from those of PE1 and PE1-OR6. In addition, the first oxidation of PE1-OR4 is much more reversible than those of PE1 and PE1-OR6. Therefore, in addition to the electro-donating influence of the alkoxyl groups, we suggest that PE1-OR4's negatively shifted redox potentials as well as the reversible oxidation may also be attributed to the wrapping alkoxyl chains. This suggestion agrees well with the results observed for PE1-OR6. Because the PE1-OR6 simulation did not suggest the wrapping phenomenon, it is reasonable to observe that the electrochemical behaviors of PE1-OR6 remain similar to those of PE1 porphyrin.

Because of free-base porphyrins were used in the simulations, it is of interest to observe the effect of the cental metal. Figure 4 compares the CVs of (zinc) PE1-OR4 and free-base PE1-OR4. The redox potentials of free-base PE1-OR4 are listed in Table 2. As shown in the figure and the table, removing the central metal ion from PE1-OR4 seem only to shift the redox potential positively. For the first porphyrin-ring reductions, the reactions are *qusai*-reversible for the zinc and the free-base porphyrins. The potentials, however, shift from PE1-OR4's -1.47 V to free-base PE1-OR4's -1.22 V. For the first porphyrin-ring oxidations, the reaction is *qusai*-reversible for PE1-OR4. Unfortunately, reversibility of free-base PE1-OR4's first oxidation is difficult to determine because the reaction is very close to the detection limit of the solvent system. Consequently, we determine the oxidation potential by differential pulse voltammetry. Nevertheless, a similar positive shift is also observed. The oxidation potentials shift from PE1-OR4's +0.85 V to free-base PE1-OR4's +1.11 V. This phenomenon is consistent with the literature reports [25]. As for the carboxylic acid reduction, the redox couples do not seem to be sensitive to the removal of the central metal ion.

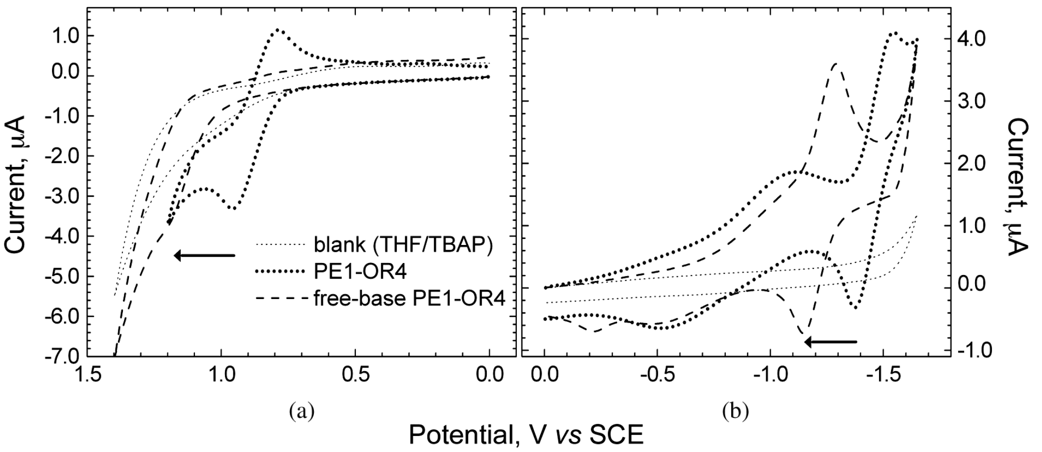

Fig. 4. Cyclic voltammograms of 1.0 mM of PE1-OR4 (bold dotted lines), and free-base PE1-OR4 (dash lines) in THF/0.1 M TBAP (thin dotted lines) solutions. The arrows indicate the potential differences between the zinc and the free-base porphyrins

Finally, it is worth mentioning that changing the lengths of the alkoxyl chains would not have a significant impact on the redox properties of alkoxyl-wrapped porphyrins. We have recently reported that shortening the alkoxyl groups from 12 carbons to 8 and to 4 carbons did not generate any sifnificant changes in the UV-visible absorptions, fluorescent emissions, and the redox behaviors of the LD14 porphyrins, a push-pull version of PE1-OR4 [17b]. Molecular simulations were carried out in the said report and the results suggested that, despite the alkoxyl chains becoming shorter, the tendency to wrap around the porphyrin core remained the same for all versions of the LD14 porphyrins.

CONCLUSION

We demonstrated that the first reduction reaction of PE1 porphyrins is actually the reduction of the anchoring carboxylic proton. We also showed that the electrochemical behaviors of a zinc porphyrin can be significantly affected by wrapping the porphine core structure with long alkyl chains.

Acknowledgements

This work was supported by the National Science Council of Taiwan.

REFERENCES

1. a) Grätzel M. *Nature*. 2001; **414**: 338–344. b) O'Regan B and Gratzel M. *Nature*. 1991; **353**: 737–740.
2. Nazeeruddin MK, Zakeeruddin SM, Humphry-Baker R, Jirousek M, Liska P, Vlachopoulos N, Shklove VR, Fischer CH and Grätzel M. *Inorg. Chem.* 1999; **38**: 6298–6305.
3. Hamann TW, Jensen RA, Martinson ABF, Ryswykac HV and Hupp JT. *Energy Environ. Sci.* 2008; **1**: 66–78.
4. Nazeeruddin MK, De Angelis F, Fantacci S, Selloni A, Viscardi G, Liska P, Ito S, Takeru B and Grätzel M. *J. Am. Chem. Soc*. 2005; **127**: 16835–16847.
5. Grätzel M. *Inorg. Chem*. 2005; **44**: 6841–6851.
6. a) Chen CY, Wang M, Li JY, Pootrakulchote N, Alibabaei L, Ngocle CH, Decoppet JD, Tsai JH, Grätzel C, Wu CG, Zakeeruddin SM and Grätzel M. *ACS Nano*. 2009; **3**: 3103–3109. b) Kuang D, Klein C, Snaith H J, Moser JE, Humphry-Baker R, Comte P, Zakeeruddin SM and Grätzel M. *Nano Lett*. 2006; **6**: 769–773.
7. a) Imahori H, Umeyama T, Ito S. *Acc. Chem. Res.* 2009; **42**: 1809–1818. b) Martinez-Diaz MV, de la Torrea G and Torres T. *Chem. Commun*. 2010; **46**: 7090–7108.
8. a) Mathew S, Iijima H, Toude Y, Umeyama T, Matano Y, Ito S, Tkachenko NV, Lemmetyinen H and Imahori H, *J. Phys. Chem. C.* 2011; **115**: 14415–14424. b) Kira A, Matsubara Y, Iijima H, Umeyama T, Matano Y, Ito S, Niemi M, Tkachenko NV, Lemmetyinen H and Imahori H. *J. Phys. Chem. C.* 2010; **114**: 11293–11304.
9. a) Lee CH, Chitre K and Galoppini E. *J. Chin. Chem. Soc*. 2010; **57**: 1103–1110. b) Lee CH and Galoppini E. *J. Org. Chem*. 2010; **75**: 3692–3704.
10. Campbell WM, Jolley KW, Wagner P, Wagner K, Walsh PJ, Gordon KC, Schmidt-Mende L, Nazeeruddin MK, Wang Q, Grätzel M and Officer DL. *J. Phys. Chem. C*. 2007; **111**: 11760–11762.
11. a) Yella A, Lee HW, Tsao HN, Yi C, Chandiran AK, Nazeeruddin MK, Diau EWG, Yeh CY, Zakeeruddin SM and Grätzel M. *Science*, 2011; **334**: 629–634. b) Bessho T, Zakeeruddin SM, Yeh CY, Diau EWG and Grätzel M. *Angew. Chem. Int. Ed*. 2010; **49**: 6646–6649.
12. a) Park SW, Hwang DS, Kim DY, Kim D. *J. Chin. Chem. Soc*. 2010; **57**: 1111–1118. b) Ishida M, Park SW, Hwang D, Koo YB, Sessler JL, Kim DY and Kim D. *J. Phys. Chem. C*. 2011; **115**: 19343–19354.

13. Biroli AO, Tessore F, Pizzotti M, Biaggi C, Ugo R, Caramori S, Aliprandi A, Bignozzi CA, De Angelis F, Giorgi G, Licandro E and Longhi E. *J. Phys. Chem. C*. 2011; **115**: 23170–23182.
14. a) Lin CY, Lo CF, Luo L, Lu HP, Hung CS and Diau EWG. *J. Phys. Chem. C*. 2009; **113**: 755–764. b) Lo CF, Luo L, Diau EWG, Chang IJ and Lin CY. *Chem. Commun*. 2006: 1430–1432.
15. Lin CY, Wang YC, Hsu SJ, Lo CF and Diau EWG. *J. Phys. Chem. C*. 2010; **114**: 687–693.
16. Lo CF, Hsu SJ, Wang CL, Cheng YH, Lu HP, Diau EWG and Lin CY. *J. Phys. Chem. C*. 2010; **114**: 12018–12023.
17. a) Chang YC, Wang CL, Pan TY, Hong SH, Lan CM, Kuo HH, Lo CF, Hsu HY, Lin CY and Diau EWG. *Chem. Commun*. 2011; **47**: 8910–8912. b) Wang CL, Lan CM, Hong SH, Wang YF, Pan TY, Chang CW, Kuo HH, Kuo MY, Diau EWG and Lin CY. *Energy Environ. Sci.* 2012; **5**: 6933–6940. c) Lan CM, Wu HP, Pan TY, Chang CW, Chen CT, Wang CL, Lin CY and Diau EWG. *Energy Environ. Sci*. 2012; **5**: 6460–6464.
18. Wang CL, Chang YC, Lan CM, Lo CF, Diau EWG and Lin CY. *Energy Environ. Sci*., 2011; **4**: 1788–1795.
19. Wu CH, Hong SH, Kuo HH, Chu YY, Diau EWG and Lin CY, *Chem. Commun.* 2012; **48**: 4329–4331.
20. *Purification of laboratory chemicals, 3^rd^ ed.*, Perrin DD and Armarego WLF. (Eds.) Pergamon Press: Oxford, 1988.
21. Lin CY, McGlashen ML, Hu S, Shim YK, Smith KM and Spiro TG. *Inorg. Chim. Acta.* 1996; **252**: 179–184.
22. Hu S, Lin CY, Blackwood Jr. ME, Mukherjee A and Spiro TG. *J. Phys. Chem*. 1995; **99**: 9694–9701.
23. Silvester DS, He W, Aldous L, Hardacre C and Richard GC, *J. Phys. Chem. C*. 2008; **112**: 12966–12973.
24. *Materials Studio*. *Accelrys Materials Studio*, v 4.2, Accelrys Inc: San Diego, CA, 2006.
25. a) For the reviews: Kadish KM, Caemelbecke EV and Royal G. In *The Porphyrin Handbook*, Vol. 8, Kadish KM, Smith KM and Guilard G. (Eds.) Academic Press: New York, 2000. b) For the database of porphyrins redox potentials in nonaqueous media: Kadish KM, Royal G, Caemelbecke EV and Gueletti L. In *The Porphyrin Handbook*, Vol. 9, Kadish KM, Smith KM and Guilard G. (Eds.) Academic Press: New York, 2000.